

Advanced 3D Monte Carlo Algorithms for Biophotonic and Medical Applications

Lewis McMillan



University of
St Andrews

This thesis is submitted in partial fulfilment for the degree of
PhD
at the
University of St Andrews

March 2019

Declaration

I, Lewis McMillan, hereby certify that this thesis, which is approximately ***** words in length, has been written by me, that it is the record of work carried out by me, or principally by myself in collaboration with others as acknowledged, and that it has not been submitted in any previous application for a higher degree.

I was admitted as a research student in September 2015 and as a candidate for the degree of PhD in September 2015; the higher study for which this is a record was carried out in the University of St Andrews between 2015 and 2019.

Date Signature of candidate

I hereby certify that the candidate has fulfilled the conditions of the Resolution and Regulations appropriate for the degree of PhD in the University of St Andrews and that the candidate is qualified to submit this thesis in application for that degree.

Date Signature of supervisor

Date Signature of supervisor

Abstract

Lorem ipsum dolor sit amet, consectetur adipiscing elit. Ut purus elit, vestibulum ut, placerat ac, adipiscing vitae, felis. Curabitur dictum gravida mauris. Nam arcu libero, nonummy eget, consectetur id, vulputate a, magna. Donec vehicula augue eu neque. Pellentesque habitant morbi tristique senectus et netus et malesuada fames ac turpis egestas. Mauris ut leo. Cras viverra metus rhoncus sem. Nulla et lectus vestibulum urna fringilla ultrices. Phasellus eu tellus sit amet tortor gravida placerat. Integer sapien est, iaculis in, pretium quis, viverra ac, nunc. Praesent eget sem vel leo ultrices bibendum. Aenean faucibus. Morbi dolor nulla, malesuada eu, pulvinar at, mollis ac, nulla. Curabitur auctor semper nulla. Donec varius orci eget risus. Duis nibh mi, congue eu, accumsan eleifend, sagittis quis, diam. Duis eget orci sit amet orci dignissim rutrum.

Nam dui ligula, fringilla a, euismod sodales, sollicitudin vel, wisi. Morbi auctor lorem non justo. Nam lacus libero, pretium at, lobortis vitae, ultricies et, tellus. Donec aliquet, tortor sed accumsan bibendum, erat ligula aliquet magna, vitae ornare odio metus a mi. Morbi ac orci et nisl hendrerit mollis. Suspendisse ut massa. Cras nec ante. Pellentesque a nulla. Cum sociis natoque penatibus et magnis dis parturient montes, nascetur ridiculus mus. Aliquam tincidunt urna. Nulla ullamcorper vestibulum turpis. Pellentesque cursus luctus mauris.

Acknowledgements

Lorem ipsum dolor sit amet, consectetur adipiscing elit. Ut purus elit, vestibulum ut, placerat ac, adipiscing vitae, felis. Curabitur dictum gravida mauris. Nam arcu libero, nonummy eget, consectetur id, vulputate a, magna. Donec vehicula augue eu neque. Pellentesque habitant morbi tristique senectus et netus et malesuada fames ac turpis egestas. Mauris ut leo. Cras viverra metus rhoncus sem. Nulla et lectus vestibulum urna fringilla ultrices. Phasellus eu tellus sit amet tortor gravida placerat. Integer sapien est, iaculis in, pretium quis, viverra ac, nunc. Praesent eget sem vel leo ultrices bibendum. Aenean faucibus. Morbi dolor nulla, malesuada eu, pulvinar at, mollis ac, nulla. Curabitur auctor semper nulla. Donec varius orci eget risus. Duis nibh mi, congue eu, accumsan eleifend, sagittis quis, diam. Duis eget orci sit amet orci dignissim rutrum.

Nam dui ligula, fringilla a, euismod sodales, sollicitudin vel, wisi. Morbi auctor lorem non justo. Nam lacus libero, pretium at, lobortis vitae, ultricies et, tellus. Donec aliquet, tortor sed accumsan bibendum, erat ligula aliquet magna, vitae ornare odio metus a mi. Morbi ac orci et nisl hendrerit mollis. Suspendisse ut massa. Cras nec ante. Pellentesque a nulla. Cum sociis natoque penatibus et magnis dis parturient montes, nascetur ridiculus mus. Aliquam tincidunt urna. Nulla ullamcorper vestibulum turpis. Pellentesque cursus luctus mauris.

Contents

Declaration	iii
Abstract	v
Acknowledgements	vii
Abbreviations	ix
List of Figures	x
1 Introduction	1
1.1 Monte Carlo Method	2
1.2 Synopsis and Thesis Objectives	4
Appendix A Fresnel Reflections	9
Appendix B Detected Light Fluence Tracking Method	13

Abbreviations

CDF cumulative distribution function.

MCRT Monte Carlo radiation transfer.

PDF probability density function.

List of Figures

- 1.1 Sample Buffon needle experiment. 100 needles are dropped on a 10×10 cm area with lines spaced 1.5 cm apart. If a needle lands on a line it is recorded and coloured blue, else it is red. This simulation gave a value of $\pi \approx 3.10$.
- 1.2 Illustration of the rejection method for determining π from the area of a circle inscribed within a square. The ratio of the area of the circle to the square is $\frac{\pi}{4}$. Thus the ratio of darts landing in the circle to those that land outside the circle is $\pi \approx \frac{4N_{inner}}{N_{total}}$, where N_{total} is the total number of darts, and N_{inner} is the total number of darts that land in the circle. Using 200 darts gave a value of $\pi \approx 3.12$.
- 1.3 Example of randomly sampling from a spectrum. Figure shows 100 random samples drawn to recreate a solar spectrum.
- 1.4 Computer generated imagery using ray tracing. The Monte Carlo method is used to “compute radiance along ray paths between lights and the camera”, to generate CGI images [23].

- A.1 Geometry for reflection of light at a refractive change boundary. I is incident light, R is the reflected light, and N is a normal to the surface. Here, θ is the angle of incidence which is equal to the angle of reflection.
- A.2 Geometry of light refraction and reflections.

- B.1 Example of the push and pop operation on a stack. The first operation add the integer 2 to the stack. The second operation push 7 to the stack. The last operation pops the 7 from the stack.

Chapter 1

Introduction

The advent of the computer in the last 80 years has been a boon for society. Increasing computing power is easily available, allowing higher-quality research, and research into topics once thought beyond human computation. One topic where computers have revolutionised is medicine. Computers have enabled advances in many areas including drug discovery [1, 2], patient diagnoses [3, 4], and better imaging modalities [5, 6]. One particular area of focus where computers are or will be heavily used is personalised medicine.

Personalised medicine is where instead of a patient being treated with what works on an “average” patient, the treatment is tailored specifically for the patient. This entails having fine grained knowledge of the patient down to the genome level, to understand how various drugs or treatments will affect the patient. One particular area of research in personalised medicine is into the so called “digital twin”. A digital twin as defined by A. El Saddik [7]:

“A digital twin is a digital replica of a living or non-living physical entity.”

Digital twins are currently heavily used in engineering to predict when various machinery will need to undergo maintenance. Digital twins operate by modelling their physical counterpart. This model is updated via information from their physical counterpart which allows the digital twin predict it’s physical counterparts future behaviour. Companies like Phillips use this in their MRI machines to help schedule downtime, and predict which parts the engineer will need on site, both of which minimises the downtime of the machine which is import for the hospital/clinic [8].

At the heart of the digital twin method, is the ability to accurately model the object or living thing being studied. This can be straightforward when the twin in question is a machine, as sensors can usually be attached to the various components to get feed back on the machines operation. Machines also have the bonus of (normally) be completely understood so that modelling them is usually easy. However, this is not as straightforward when dealing with biology. First, we still do not have a complete understanding of the biology within humans. Therefore, modelling a human accurately is not possible as various assumptions and approximations have to be made. Second, to get accurate information on what is happening inside a patient, generally either ionising radiation needs to be used, or cameras inserted into the patient. Both of these cannot be done for indefinite periods without causing harm or discomfort to the patient. Therefore, continuous information on the inner functions of the body is not possible. One area where information is more readily available is the skin. Information on the skin function or dysfunction is normally diagnosed with light. Light is also used in various treatments such as photodynamic therapy and tissue ablation, over various internal and external sites on the body. Lights interaction over the whole spectrum, from the UV to the infrared, is readily modelled

with techniques such as Monte Carlo radiation transfer (MCRT). MCRT allows a digital twin model of the individual patient skin to be simulated. This can then be used to tailor treatment regimes for the individual patient, or to predict treatment outcomes for specific patients. The use of simulations techniques like MCRT allow testing *in-silico*, can negate the need to test on humans or animals.

This thesis concerns the development of various MCRT models to help diagnose, optimise treatments and help predict which imaging modalities may be better.

1.1 Monte Carlo Method

The Monte Carlo method is a numerical analysis technique based upon random numbers, which are used to calculate unknown variables in problems [9, 10].

The earliest use of the method is in Buffon’s needle experiment of the 18th century [11–13]. Buffon asked the question;

“Suppose we have a floor made of parallel strips of wood, each the same width, and we drop a needle onto the floor. What is the probability that the needle will lie across a line between two strips?”

The solution to this question is: for a needle length l , strip separation s , where x is the distance from the needle to the closest line, and θ is the angle of the needle with respect to the wood strips. Then using a simple geometrical argument, a needle crosses a strip if $x \leq \frac{l}{2} \sin \theta$.

x is distributed uniformly in $[0, \frac{s}{2}]$, and θ in $[0, \frac{\pi}{2}]$. Therefore the probability density function for x is $p(x) = \frac{2}{s}$, and θ is $p(\theta) = \frac{2}{\pi}$. The probability density function (PDF), is a function of a variable that gives probability for a variable to a take a given value. The PDF is normalised over the whole range of the variable, in this case x , and θ . Thus, as x and θ are independent variables, giving a joint probability of $p(x, \theta) = \frac{4}{s\pi}$. So the probability of a needle of length l ($l < s$) is:

$$P = \int_0^{\frac{\pi}{2}} \int_0^{\frac{l}{2} \sin \theta} \frac{4}{s\pi} dx d\theta = \frac{2l}{s\pi} \quad (1.1)$$

Equation (1.1) can be used to carry out a Monte Carlo estimation of π . A simple rearrangement yields: $\pi = \frac{2l}{sP}$ where P is the ratio of needles crossing the line to the total number dropped. Laplace was the first to suggest that Buffon’s needle experiment could be used to estimate π [12]. Figure 1.1 shows an example of a simulation of Buffon’s needle experiment.

There are various different approaches to using the Monte Carlo method to obtain randomly sampled variables. One analytical way of achieving this is the inverted sampling method. The inverted sampling method can be summarised by the following steps for drawing a sample X_i from an arbitrary PDF $p(x)$:

1. Compute the cumulative distribution function (CDF) $P(x) = \int_0^x p(x') dx'$
2. Compute the inverse $P^{-1}(x)$
3. Obtain a uniformly distributed random number ξ
4. Finally, compute $X_i = P^{-1}(\xi)$

If a given problem cannot use the inverted sampling method, as it may not be possible to get a PDF or analytically invert the CDF, then the rejection method can be used. The rejection method is essentially a dart throwing method. This means that points are drawn and compared to the function. If the point lies under the function then the point is accepted, if it lies above the function then it is rejected. For example, if a function, $f(x)$ that does not have an analytical

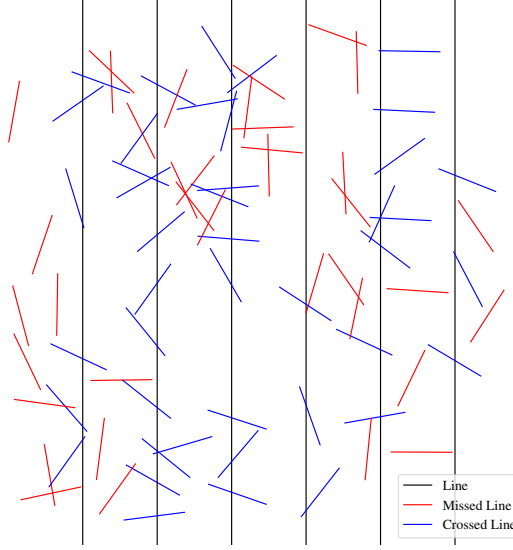


Figure 1.1: Sample Buffon needle experiment. 100 needles are dropped on a 10×10 cm area with lines spaced 1.5 cm apart. If a needle lands on a line it is recorded and coloured blue, else it is red. This simulation gave a value of $\pi \approx 3.10$.

PDF, we can use a PDF $p(x)$ such that $f(x) < cp(x)$ where c is a constant. Therefore sampling from $p(x)$, and if the sampled point lies under $f(x)$ it is accepted, else it is rejected. Figure 1.2 shows an example of this process.

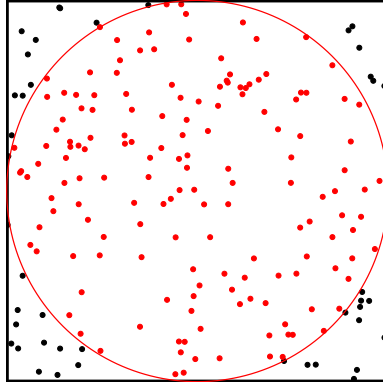


Figure 1.2: Illustration of the rejection method for determining π from the area of a circle inscribed within a square. The ratio of the area of the circle to the square is $\frac{\pi}{4}$. Thus the ratio of darts landing in the circle to those that land outside the circle is $\pi \approx \frac{4N_{\text{inner}}}{N_{\text{total}}}$, where N_{total} is the total number of darts, and N_{inner} is the total number of darts that land in the circle. Using 200 darts gave a value of $\pi \approx 3.12$

One common use of the Monte Carlo method, is to randomly sample from a spectrum. To generate a random sample from a spectrum, first the CDF of the spectrum must be calculated. This is done by first normalising the PDF, where the PDF in this case is the spectrum it self. It

is normalised such that the sum of the PDF is unity. The CDF is then just the cumulative sum of the PDF. Then using the above method as described above, a random number is drawn, ξ , and the bracketing values in the CDF are found. We then interpolate to get the x and y values corresponding to ξ . Figure 1.3 shows the result of this process for 100 random samples.

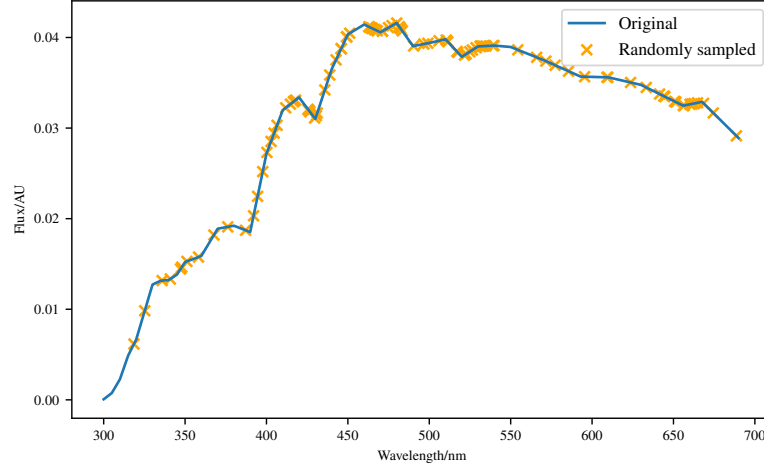


Figure 1.3: Example of randomly sampling from a spectrum. Figure shows 100 random samples drawn to recreate a solar spectrum.

The Monte Carlo method is used in various different disciplines. Ranging from use in the financial sector to analyse investments and stocks by simulating the sources of uncertainty which affect their values [14, 15], use in statistical analysis [16], and in modern computer generated images (see Fig. 1.4) [17, 18]. It is also widely used in astronomy [19, 20] and medicine [21, 22], to simulate the propagation of radiation through scattering (turbid) media. This technique, MCRT, is what makes up the bulk of this thesis and is described in depth in the following sections.

1.2 Synopsis and Thesis Objectives

Chapter 2 details the MCRT method that is used for the bulk of this thesis. Presented in this chapter are details of the algorithm and various code details that underpin the whole thesis. Details of speed up techniques such as parallelisation are also presented. Finally the code is validated against other results.

Chapter 3 details the tissue ablation model. Discussion of the individual components of the model, alongside validation of the model against theoretical and experimental evidence is presented.

Chapter 4 presents an adaptation to the regular Monte Carlo model so that it can model wave like properties of photons including diffraction and interference. The new algorithm is validated against several theoretical expressions and experimental data. Finally the algorithm is used to compare Bessel beams and Gaussian beam in highly turbid media, to determine which beam preforms better.

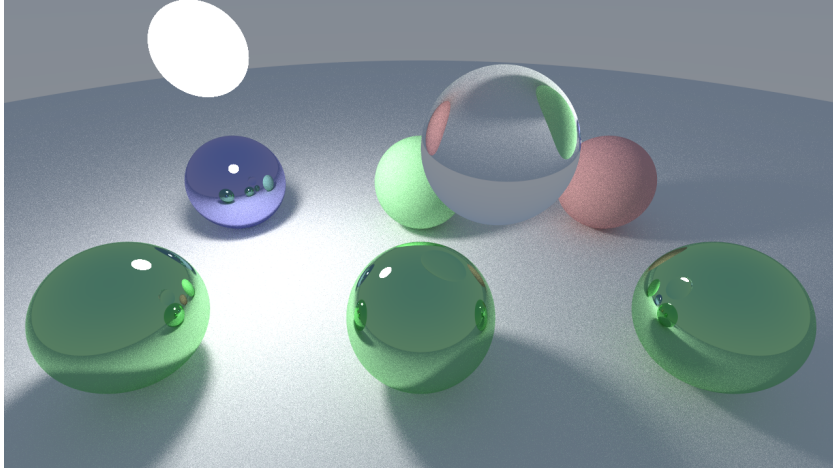


Figure 1.4: Computer generated imagery using ray tracing. The Monte Carlo method is used to “compute radiance along ray paths between lights and the camera”, to generate CGI images [23].

Chapter 5 details the modelling of a novel biomarker for cardiovascular disease, autofluorescence. The theoretical groundwork for the biomarker is outlaid, along with discussion of how MCRT can model fluorescence. Presented alongside this is *ameombaMCRT*, a Monte Carlo radiation transfer simplex algorithm used to determine concentrations of fluorophores in different layers of tissue for a given spectrum.

Finally, chapter 6 concludes this thesis and presents possible future avenues of research that could be undertaken.

Appendices

Appendix A

Fresnel Reflections

In order to be able to accurately model the paths that light take in a medium where the refractive indices varies, Fresnel reflections and refractions must be modelled. To model these reflections and refractions in a simulation we calculate the Fresnel coefficients. Equations (A.1) to (A.3) shows the equations for calculating these for s and p polarised light, and unpolarised light (Eq. (A.3)).

$$R_s = \left| \frac{n_1 \cos \theta_i - n_2 \cos \theta_t}{n_1 \cos \theta_i + n_2 \cos \theta_t} \right|^2 \quad (\text{A.1})$$

$$R_p = \left| \frac{n_1 \cos \theta_t - n_2 \cos \theta_i}{n_1 \cos \theta_t + n_2 \cos \theta_i} \right|^2 \quad (\text{A.2})$$

$$R_{eff} = \frac{1}{2} (R_s + R_p) \quad (\text{A.3})$$

Where:

θ_i and θ_t are the angle of incidence and angle of transmission respectively,

see Eqs. (A.4) and (A.5) and Figs. A.1 and A.2;

n_1 and n_2 are the refractive indices of the current medium and the transmission medium [-];

R_s and R_p are the reflectance coefficients for s and p polarised light respectively [-];

finally, R_{eff} is the effective reflective coefficient for unpolarised light [-].

$$\sin \theta_t = \frac{n_1}{n_2} \sin \theta_i \quad (\text{A.4})$$

$$\cos \theta_t = \sqrt{1. - \sin \theta_t^2} \quad (\text{A.5})$$

R_{eff} gives a probability of reflection or refraction for a ray of light with an angle of incidence θ_i .

To calculate the angles of reflection and refraction, a vector form of Snell's law is used. Using the geometry illustrated in Fig. A.1 one can see that:

$$I = A + B \quad (\text{A.6})$$

$$R = A - B \quad (\text{A.7})$$

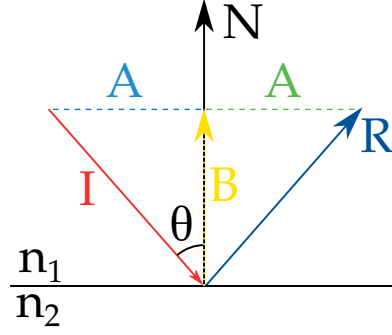


Figure A.1: Geometry for reflection of light at a refractive change boundary. I is incident light, R is the reflected light, and N is a normal to the surface. Here, θ is the angle of incidence which is equal to the angle of reflection.

$$B = \cos(\theta) \cdot N \quad (\text{A.8})$$

Therefore, substituting Eq. (A.8) into Eqs. (A.6) and (A.7) and rearranging yields:

$$I = A + \cos(\theta) \cdot N \quad (\text{A.9})$$

$$R = A - \cos(\theta) \cdot N \quad (\text{A.10})$$

$$\therefore R = I - 2(N \cdot I)N \quad (\text{A.11})$$

Where R gives the vector for a ray of light that has undergone reflection. Next we treat the transmission case. Figure A.2 gives the geometry for the situation, where the circle is a unit circle.

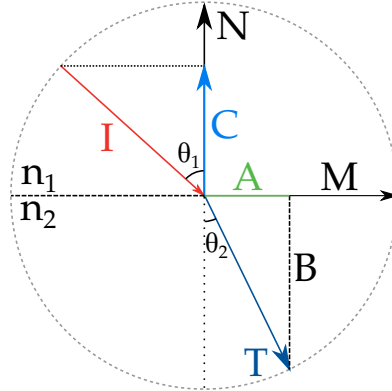


Figure A.2: Geometry of light refraction and reflections.

Again, one can deduce the following using trigonometry and Fig. A.2:

$$T = A + B \quad (\text{A.12})$$

$$A = \sin(\theta_2) M \quad (\text{A.13})$$

$$B = \cos(\theta_2) (-N) \quad (\text{A.14})$$

$$C = \cos(\theta_1) N \quad (\text{A.15})$$

$$M = \frac{I + C}{\sin(\theta_1)} \quad (\text{A.16})$$

Substituting Eqs. (A.13) to (A.16) into Eq. (A.12), using Snell's law (Eq. (A.21)), and rearranging yields:

$$T = A + B \quad (\text{A.17})$$

$$= M \sin \theta_2 - N \cos \theta_2 \quad (\text{A.18})$$

$$= \frac{I + C}{\sin \theta_1} \sin \theta_2 - N \cos \theta_2 \quad (\text{A.19})$$

$$= \frac{(I + \cos \theta_1 N) \sin \theta_2}{\sin \theta_1} - N \cos \theta_2 \quad (\text{A.20})$$

$$\frac{\sin \theta_1}{\sin \theta_2} = \frac{\eta_1}{\eta_2} \quad (\text{A.21})$$

$$\therefore T = \frac{\eta_1}{\eta_2} (I + \cos \theta_1 N) - N \cos \theta_2 \quad (\text{A.22})$$

$$T = \eta + (\eta c_1 - c_2) N \quad (\text{A.23})$$

Where Eq. (A.22) can be simplified by defining the following expressions:

$$c_1 = N \cdot I \quad (\text{A.24})$$

$$c_2 = \sqrt{1 - \eta^2(1 - c_1^2)} \quad (\text{A.25})$$

$$\eta = \frac{\eta_1}{\eta_2} \quad (\text{A.26})$$

To apply Eqs. (A.11) and (A.23) to our voxel model, the algorithm checks if there is a change in refractive index whenever a photon packet moves into a new voxel. If there is a change of refractive index the packet is placed on the surface of the voxel, and the algorithm calculates the surface normal of the voxel the light has hit and uses the above equations to calculate R_{eff} . With R_{eff} calculated a random number, ξ , is drawn. If ξ is less than R_{eff} then the photon packet is reflected, else then the packet is refracted into the new voxel. The new direction vectors are set according to Eqs. (A.11) and (A.23) and the packet is propagated as normal.

Appendix B

Detected Light Fluence Tracking Method

Most the fluence graphs presented in this thesis shows the fluence of the incident light throughout the simulated medium. However, there are problems where tracking the fluence of the detected light maybe useful, though this quantity is not straight forward to track. The current method of tracking fluence is to add pathlengths, calculated as the packet moves from voxel to voxel to a 3D array. This method obviously cannot determine which packet will be detected before the packet is detected, therefore a new method must be devised. This new method tracks the coordinates, direction vectors, random optical distance and fluorescent source of the packet using a stack. A stack is a commonly used abstract data structure, and is a collection of elements. In this case the elements are the coordinates, direction vectors, optical distance and fluorescent source. A stack has two main operations, pop and push. The push operation adds a new element to the collection, and the pop operation removes the most recently added element from the collection. This is known as last in first out (LIFO). Figure B.1 shows these two operations in action.

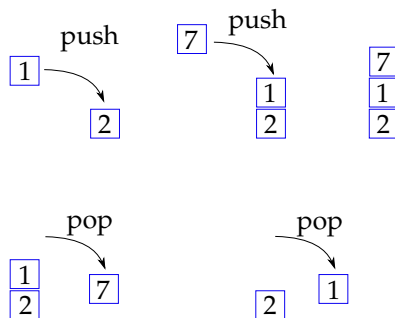


Figure B.1: Example of the push and pop operation on a stack. The first operation add the integer 2 to the stack. The second operation push 7 to the stack. The last operation pops the 7 from the stack.

The progress of each packet is pushed onto the stack, as it is propagated through the simulated medium. As mentioned above the packets coordinates, direction vectors, optical depth, and fluorescent source are the quantities pushed to the stack. These quantities are pushed to stack every time an interaction event occurs. When a packet is terminated, either via absorption or

it leaving the medium, the packets details are removed from the stack. This occurs unless the packet is detected. If the packet is detected then the information remains on the stack. This whole process repeats until all the packets have been run. Once all the packets have been run, the packets are “replayed”. This is achieved by popping the information off the stack and passed to the `inttau2` routine. The packet is then propagated again, this time recording the fluence as done in most of the chapters in this thesis.

Bibliography

- [1] J. Åqvist, C. Medina, and JE. Samuelsson. A new method for predicting binding affinity in computer-aided drug design. *Protein Engineering, Design and Selection*, 7(3):385–391, 1994.
- [2] M.A Lill and M.L Danielson. Computer-aided drug design platform using pymol. *Journal of computer-aided molecular design*, 25(1):13–19, 2011.
- [3] S. Liu, S. Liu, W. Cai, S. Pujol, R. Kikinis, and D. Feng. Early diagnosis of alzheimer’s disease with deep learning. In *2014 IEEE 11th international symposium on biomedical imaging (ISBI)*, pages 1015–1018. IEEE, 2014.
- [4] W. Sun, B. Zheng, and W. Qian. Computer aided lung cancer diagnosis with deep learning algorithms. In *Medical imaging 2016: computer-aided diagnosis*, volume 9785, page 97850Z. International Society for Optics and Photonics, 2016.
- [5] R.A Brooks and G. Di Chiro. Principles of computer assisted tomography (cat) in radiographic and radioisotopic imaging. *Physics in Medicine & Biology*, 21(5):689, 1976.
- [6] S. Al-Janabi, A. Huisman, and P.J Van Diest. Digital pathology: current status and future perspectives. *Histopathology*, 61(1):1–9, 2012.
- [7] A. El Saddik. Digital twins: The convergence of multimedia technologies. *IEEE MultiMedia*, 25(2):87–92, 2018.
- [8] H. van Houten. The rise of the digital twin: how healthcare can benefit. In <https://www.philips.com/a-w/about/news/archive/blogs/innovation-matters/20180830-the-rise-of-the-digital-twin-how-healthcare-can-benefit.html>. Philips, Aug 2018.
- [9] E.D Cashwell and C.J Everett. A practical manual on the monte carlo method for random walk problems. 1959.
- [10] D.W.O Rogers and A.F Bielajew. Monte carlo techniques of electron and photon transport for radiation dosimetry. *The dosimetry of ionizing radiation*, 3:427–539, 1990.
- [11] L. Badger. Lazzarini’s lucky approximation of π . *Mathematics Magazine*, 67(2):83–91, 1994.
- [12] P. Beckmann. *A history of Pi*. St. Martin’s Griffin, 2015.
- [13] GL.L Buffon. *Histoire naturelle générale et particulière*, volume 18. de l’Imprimerie de F. Dufart, 1785.
- [14] P. Jäckel. *Monte Carlo methods in finance*. J. Wiley, 2002.

- [15] D.B Hertz. Risk analysis in capital investment. *Harvard Business Review*, 42(1):95–106, 1964.
- [16] J.V Wall and C.R Jenkins. *Practical statistics for astronomers*. Cambridge University Press, 2012.
- [17] J.T Kajiya. The rendering equation. *SIGGRAPH Comput. Graph.*, 20(4):143–150, August 1986.
- [18] R.L Cook, T. Porter, and L Carpenter. Distributed ray tracing. *SIGGRAPH Comput. Graph.*, 18(3):137–145, January 1984.
- [19] T.P Robitaille. Hyperion: an open-source parallelized three-dimensional dust continuum radiative transfer code. *Astronomy & Astrophysics*, 536:A79, 2011.
- [20] T. Harries. Torus: Radiation transport and hydrodynamics code. *Astrophysics Source Code Library*, 2014.
- [21] R.M Valentine, C.T.A Brown, K. Wood, H. Moseley, and S. Ibbotson. Monte carlo modeling of in vivo protoporphyrin ix fluorescence and singlet oxygen production during photodynamic therapy for patients presenting with superficial basal cell carcinomas. *Journal of Biomedical Optics*, 16(4):048002, 2011.
- [22] C.L Campbell, K. Wood, R.M. Valentine, C.T.A Brown, and H. Moseley. Monte carlo modelling of daylight activated photodynamic therapy. *Physics in Medicine & Biology*, 60(10):4059, 2015.
- [23] M. Pharr, W. Jakob, and G. Humphreys. *Physically based rendering: From theory to implementation*. Morgan Kaufmann, 2016.